

Analysis and Optimization of Frequency Response of Electrodynamic Speaker Driver

F. J. Gadegaard, J. H. Nielsen, M. Jensen, S. S. Søndergaard

Department of Materials and Production, Aalborg University
Fibigerstraede 16, DK-9220 Aalborg East, Denmark
Email: fgadeg17, jaconi17, mathij17, ssande17@student.aau.dk
Web page: <http://www.mechman.mp.aau.dk/>

Abstract

This project analyses an electrodynamic speaker driver from Børresen Acoustics using FE-models. Børresen Acoustics has presented two impedance peaks of unknown origin at 1625 Hz and 3979 Hz from their measurements of the frequency response of the speaker driver. The impedance peaks are suspected to be related to unwanted mechanical resonances. The speaker driver is analysed using modal and harmonic analyses with the intent of determining its frequency response. When analysing the results of the harmonic analysis of the full assembly, a radial and a concentric membrane vibration mode is identified at 1444 Hz and 4278 Hz respectively, which are believed to be the origins of the presented impedance peaks. Following the identification of the membrane vibration modes, a shape optimization of the membrane is performed with the intent to maximize the first eigenfrequency of the membrane, corresponding to the membrane vibration mode observed at 1444 Hz, by introducing a variable thickness of the membrane. The eigenfrequency of the first radial mode shape of the optimized membrane is increased by 124 %, and as a result, the following eigenfrequencies of radial mode shapes are increased. It was not possible to increase the eigenfrequency of the concentric mode shape, however, all membrane eigenfrequencies have been shifted outside the upper limit of the operating range of the speaker driver of 2500 Hz.

Keywords: FEA, Composites, Modal analysis, Harmonic analysis, Shape optimization

1. Introduction

The danish based company Børresen Acoustics has developed and patented an electrodynamic speaker driver without iron components. This speaker driver can be seen on Figure 1. This new construction poses great advantages over the generic speaker driver. However, with this new design, two resonance peaks, with undetermined origin, have been discovered. These are discovered by measuring the electrical impedance of the speaker driver, and are also detectable by measuring the Sound Pressure Level (SPL) of the speaker driver.

The construction of the Børresen Acoustics electrodynamic speaker driver can be seen on Figure 2. The electrical system is an electromagnetic motor with a setup of four opposing N52 neodymium ring magnets. These direct a magnetic field over two solid copper rings, which function as pole pieces, and across the narrow gap between the inner and outer magnets in which the voice coil resides. This results in a magnetic flux density of 1.1 T [1]. By running a current through the voice coil, a force perpendicular to the magnetic field is produced.



Fig. 1 Picture of Børresen Acoustics speaker driver

The mechanical system, composed of the voice coil, membrane, spider and surround, is excited by the force and thus moves the membrane. The spider and surround forms the suspension system of the speaker driver. The membrane in turn displaces air, which is perceived as sound by the human ear i.e. the acoustical system. The speaker driver is implemented in Børresen Acoustics' 2.5 way speakers, and has an operating range of 0-2500 Hz.

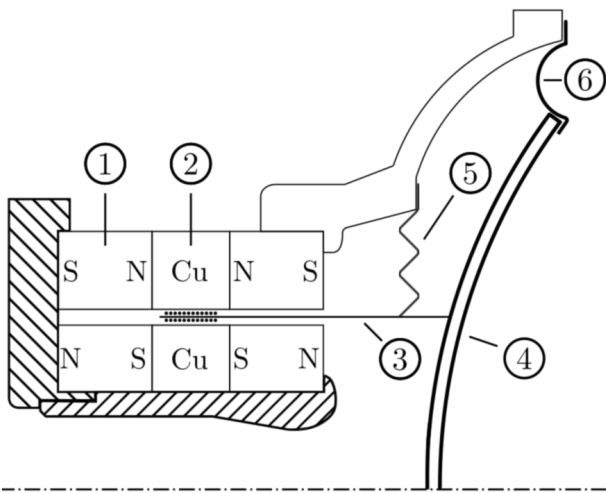


Fig. 2 Axisymmetrical illustration of Børresen Acoustics speaker driver. (1) Neodymium ring magnets (2) Copper pole pieces (3) Voice coil (4) Membrane (5) Spider (6) Surround.

The experimentally determined impedance plot, shown on Figure 3, discovers three points of interest, namely the major impedance peak at 38 Hz, and the following two minor impedance peaks at 1625 Hz and 3979 Hz. The impedance plot is a measurement of the modulus of the electrical systems impedance in interaction with the mechanical system and acoustical system.

The first impedance peak is a result of the counteracting electromagnetic force at the fundamental eigenfrequency of the mechanical system. The damping of the mechanical system and viscous damping of the acoustical system has a negligible effect on the placement of the fundamental eigenfrequency. It is believed that the second and third impedance peak observed on Figure 3, is caused by mechanical eigenfrequencies.

In an ideal scenario, the membrane of a speaker driver acts as an infinitely rigid piston. However, in the real world it will deform and have resonances, which affect the reproduction of sound. These resonances are described as membrane vibration modes, which

are divided into two classifications, namely radial and concentric modes [2]. These vibration modes can be further described using the concept of nodes [3]. Nodes are defined as locations with no oscillation and thus, a transition between positive phase and negative phase. This is exemplified on Figure 4, which depicts a radial, concentric, and a mixed mode with its corresponding nodes.

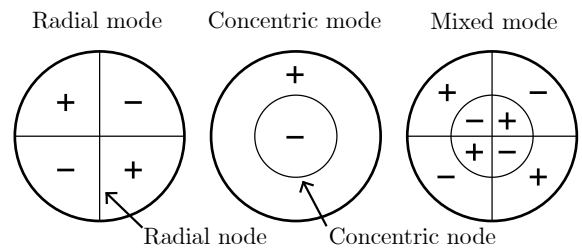


Fig. 4 Radial, concentric, and mixed membrane vibration modes with their corresponding nodes, separating the membrane into sections with positive or negative phase.

Radial modes exhibit only circumferential deformations with radial nodes forming a line that extends from the membrane center to the edge. These primarily occur at lower frequencies than concentric modes [2]. The membrane mode at the lowest eigenfrequency is a radial vibration mode containing four radial nodes, thus dividing the membrane into four sections of positive and negative phase respectively. Concentric modes exhibit only axisymmetric deformations with concentric nodes that form a circle on the membrane. The first concentric vibration mode contains one concentric node, thus dividing the membrane into two sections of positive and negative phase. The mixed membrane vibration modes are combinations of radial and concentric modes. The dynamic behavior of the vibration modes are complex compared to the desired piston mode, and contains sections which are in or out of phase with the signal to the voice coil. The resulting added or cancelled movement of the membrane is described as membrane break up.

The fundamental eigenfrequency of the speaker driver is a piston mode, in which the entirety of the membrane oscillates in phase, thus no radial nodes or concentric nodes are present. This is the result of the mass of the membrane and voice coil, and the stiffness of the suspension system. The piston mode is the vibration mode responsible for producing sound, and all other vibration modes will produce deviations from the

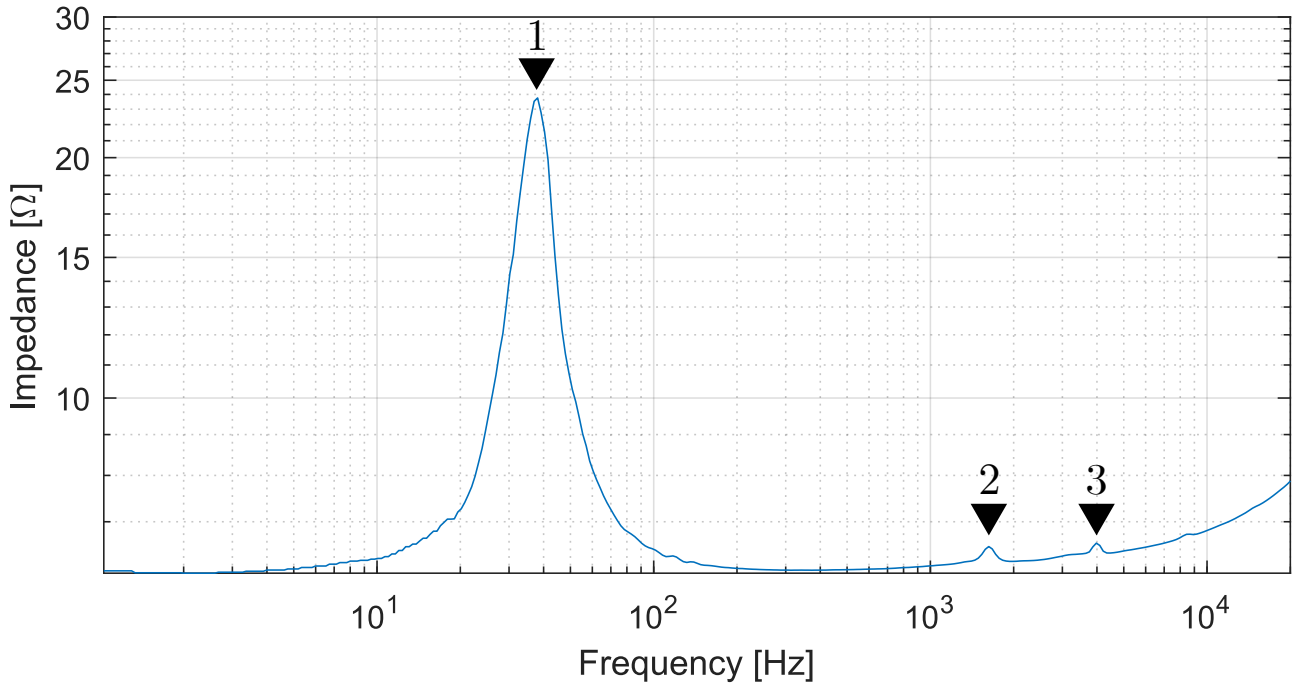


Fig. 3 Impedance plot of Børresen Acoustics speaker driver. Three distinct peaks are observed, shown by the numbering. 1: 38 Hz, 2: 1625 Hz, 3: 3979 Hz.

desired sound output, which is perceived as unwanted noise or distortion [2].

The objective of this paper is to localize and identify the origin of the presented impedance peaks, with the intent to shift these peaks outside of the operating range of the speaker driver or suppress these entirely. As the origin of the impedance peaks are suspected to be mechanical resonances, the analyses presented in the paper will be limited to the mechanical system. Allowed changes to the speaker driver are limited to the membrane and surround. Furthermore, the mechanical system will be analysed with damping effects omitted. In order to shift the impedance peaks outside of the operating range of the speaker driver, the paper will formulate a shape optimization based on the mechanical system.

1.1 Requirements

To find the best revised design, a list of requirements is stated in Table 1. These are composed of goals, restrictions, and functions. Two goals are introduced to alleviate the impedance peaks. Shift these entirely outside of the operating range of the speaker driver, as no significant effect is expected if they are only shifted inside the operating range of 2500 Hz, or reduce their amplitude. The fundamental eigenfrequency of the speaker driver must have a tolerance of 38 Hz \pm 1 Hz. This acts as a restriction and a function. Finally,

geometric constraints of the geometry of the membrane and surround are governed by the geometry of the basket and electromagnetic motor.

	Goals	Restrictions	Functions
Placements of eigenfrequencies	✓		
Amplitudes of peaks	✓		
Fundamental eigenfrequency		✓	✓
Geometric constrains		✓	

Tab. 1 Categorisation of requirements.

For a further explanation of the different requirements see appendix report section 2.1.

2. Material and Methods

Table 2 and Table 3 lists the material properties for the moving components of the speaker driver. It must be noted that the material parameters used or determined, do not necessarily correspond to those of the materials used in the Børresen Acoustics speaker driver. Thus, the obtained material parameters are associated with a degree of uncertainty. Table 2 contains the material parameters of UD-carbon fiber, CSM-carbon fiber and Nomex honeycomb. These parameters are obtained through a material analysis described in the appendix report section 3.1.

Material	E_1	E_2	E_3	ν_{12}	ν_{23}	ν_{13}	G_{12}	G_{23}	G_{13}	ρ
UD GPa	143	9.9	9.9	0.307	0.506	0.307	6.9	0.3	6.9	1580
CSM GPa	55.9	55.9	12.6	0.293	0.347	0.347	21.6	3.67	3.67	1580
Nomex MPa	0.06	0.06	79.0	0.9984	0.0002	0.0002	0.02	19.9	19.9	29

Tab. 2 Obtained material properties of the membrane constituents.

Components	Young's MPa	Poisson's ratio	Density kg m^{-3}
Surround [4]	2.76	0.48	1124.4
Spider [4][5][6]	175-1000	0.333	450
Former	91	0.36	4620
Coil	100	0.36	6500

Tab. 3 Material properties of components.

2.1 Modal and Harmonic Analyses

The components of the speaker driver are analysed using FE-analyses. The FE-analyses are performed in ANSYS Workbench using Modal Analysis, from which the eigenfrequencies and corresponding mode shapes are obtained. In order to determine the frequency response of the full assembly, a FE-analysis in ANSYS Workbench using Harmonic Response is performed. The applied excitation force for the harmonic analyses is determined to be 116 N. Further details on the calculation of the excitation force can be found in the appendix report section 4.2. Initially, the components are analysed individually, with the intent of isolating any problematic eigenfrequencies to a specific component. Thus, the mode shapes obtained for the full assembly can be compared to those obtained for the individual components, thereby allowing the origin of specific vibration modes in the full assembly to be isolated to a specific component or interaction between components. The intent of the harmonic analysis is to isolate vibration modes caused by a harmonic excitation, which results in displacement peaks associated with the membrane, and compare these to those seen in the impedance plot supplied by Børresen Acoustics. Thus, the goal is to identify any problematic eigenfrequencies and their corresponding vibration modes, and isolate their origin to a specific component. The harmonic analysis is performed by the use of mode superposition, which uses the mode shapes determined from the modal analysis. The frequency range of both analyses is 0-11 000 Hz.

A significant amount of displacement peaks, as seen on Figure 5, are the result of the contributing vibration modes of the surround and their influence on the membrane. The surround vibration modes mask the physical frequency response of the membrane by introducing nonphysical surround vibration modes associated with large displacements, which in turn affect the maximum displacement of the membrane. It is expected that the

material damping of the rubber surround will reduce or remove these displacement peaks entirely. It is chosen to narrow the frequency range to 1000-1700 Hz and 3500-4500 Hz, as seen in Figure 5, in order to reduce the concentration of surround modes on the displacement plot, and thereby allow a thorough analysis of the individual displacement peaks. The frequency ranges are chosen, such that they coincide with the impedance peak at 1625 Hz and 3979 Hz respectively.

2.2 Displacement peak identification procedure

The analysis of the displacement peaks follows a predetermined procedure to aid the correct identification of their origins. Initially, a displacement peak is identified on the displacement plot of the harmonic analysis and selected for further analysis. Hereafter, the vibration mode is analysed in the harmonic analysis at the frequency of the displacement peak. In this analysis, it might be difficult to separate the origin of the displacement peak between the components, thus why the vibration mode is also identified in the modal analysis as the mode shape at the same frequency. Here, the origin of the displacement peak is clearer. If the analysis of the displacement peak is only performed in either the modal or harmonic analysis, a possibility of false identification is highly plausible.

Two results from the following analyses are highlighted to describe this procedure. A membrane vibration mode with eight radial nodes is observed at two different frequencies of 1664 Hz and 3744 Hz, as illustrated in the overlaid boxes of Figure 6 and Figure 7. However one is excited by the surround, as shown in Figure 6, and one is truly a membrane vibration mode as shown in Figure 7. The observed membrane vibration mode at 1664 Hz in the harmonic analysis does not exist as a mode shape in the modal analysis at 1664 Hz. However the observed membrane vibration mode at 3744 Hz in the harmonic analysis does exist as a mode shape in the modal analysis at 3744 Hz. When comparing the deformation of the surround, one can identify a surround mode at 1664 Hz, which has a vibration mode with large displacements, capable of exciting the membrane in a radial vibration mode as illustrated in Figure 6. However, at 3744 Hz, the surround vibration

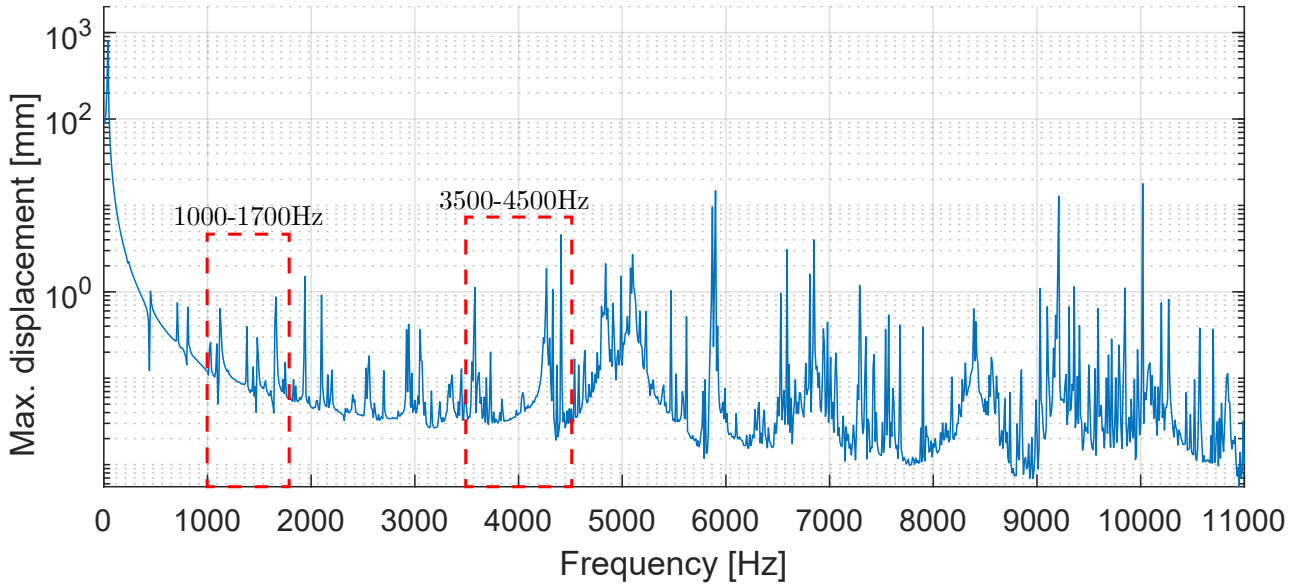


Fig. 5 Maximum displacement measured on the membrane. Narrowed frequency ranges are marked with the red boxes and assigned frequency intervals.

mode is entirely unrelated to the vibration mode of the membrane, as apparent from Figure 7, thus further supporting the conclusion from the modal analysis. Furthermore, the displacement of the membrane and surround are of the same order of magnitude.

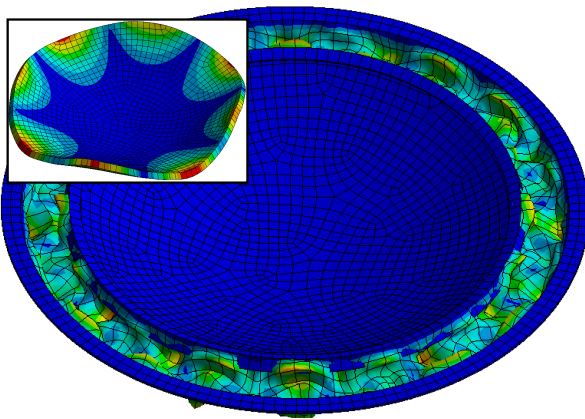


Fig. 6 Comparison of mode shapes, of vibration mode identified in the harmonic analysis of the full assembly at 1664 Hz. Membrane mode shape is isolated in overlaid box.

Thus, the apparent membrane vibration mode at 1664 Hz is deemed a surround vibration mode, and the membrane vibration mode at 3744 Hz is accepted. Finally, the modal analysis of the membrane can be utilized to evaluate whether the frequencies of the membrane vibration modes in the full assembly associated with identified displacement peaks, roughly correspond the eigenfrequencies of the membrane mode shapes determined in the modal analysis of the membrane.

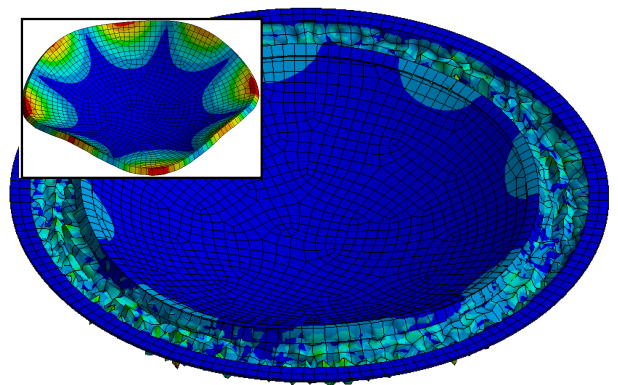


Fig. 7 Comparison of mode shapes, of vibration mode identified in the harmonic analysis of the full assembly at 3744 Hz. Membrane mode shape is isolated in overlaid box.

3. Identified displacement peaks

The full identification and analyses of displacement peaks in the analysed frequency range of 1000-1700 Hz and 3500-4500 Hz can be seen in the appendix report section 4.3.2. Only displacement peak 4 from the first frequency range and displacement peak 6 from the second frequency range is presented.

The origins of the impedance peaks presented in section 1 has been identified by the thorough analyses of the two harmonic analyses in the narrowed frequency ranges. It is proposed that the impedance peak at 1625 Hz on Figure 3 has origins in a membrane vibration mode with four radial nodes observed at 1444 Hz at peak 4, as illustrated on Figure 8. This

membrane mode shape is illustrated in Figure 10. However, the radial vibration mode is not associated with large voice coil displacements. Only the surround is affected by the membrane vibration mode, which could possibly change the characteristics of the surround. Nonetheless, the first radial membrane vibration mode is associated with significant sound radiation properties, thus why, it is of interest for the following analyses. Furthermore, it is proposed that the impedance peak at 3979 Hz on Figure 3 has origins in a membrane vibration mode with one concentric node observed at 4278 Hz at peak 6 as illustrated in Figure 9. In this membrane mode shape, which is illustrated in Figure 11, the membrane and voice coil moves in anti-phase, thus being a clear candidate for the origin of the impedance peak at 3979 Hz. As both origins of the presented impedance peaks are associated with membrane vibration modes, an optimization study of the membrane will be performed with the intent to suppress or shift the membrane eigenfrequencies outside of the operating range of the speaker driver.

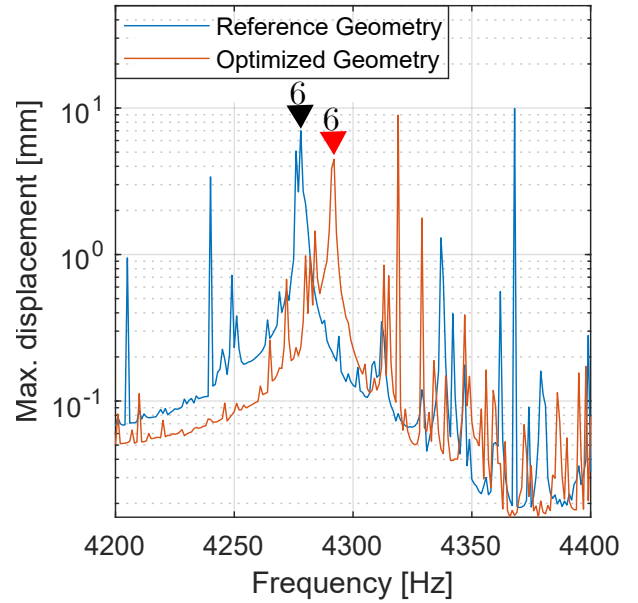


Fig. 9 Maximum displacement of the membrane as a function of frequency. Peak of interest (6) is at a frequency of 4278 Hz (black arrow) and 4292 Hz (red arrow).

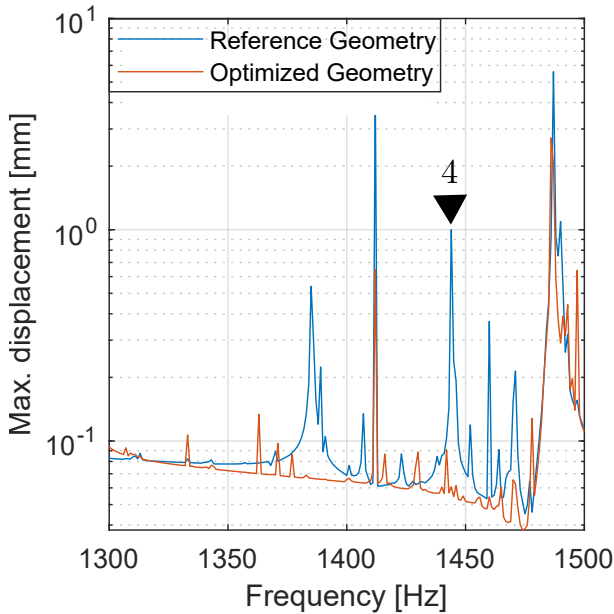


Fig. 8 Maximum displacement of the membrane as a function of frequency. Peak of interest (4) is at a frequency of 1444 Hz.

4. Optimization

The speaker driver is optimized with regards to the problematic eigenfrequencies and their corresponding mode shapes. Hence, the goal of the optimization is to perform a shape optimization of the membrane to shift the problematic vibration modes of the full assembly outside of the operating range of the speaker driver.

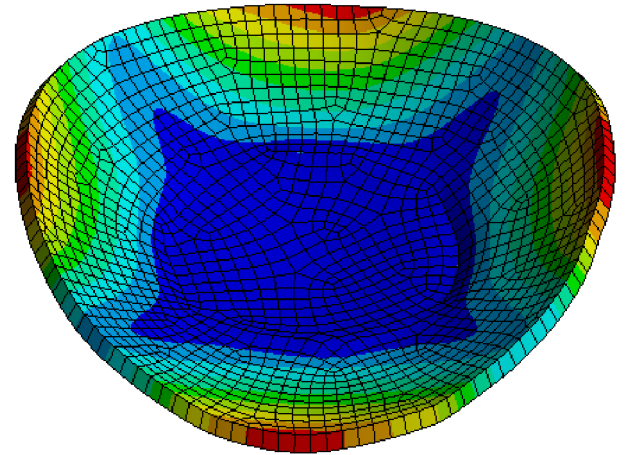


Fig. 10 Vibration mode corresponding to peak 4 at 1444 Hz.

4.1 Formulation of optimization

The membrane is optimized using a shape optimization procedure, in which the geometry of the membrane is parameterized. However, in order to facilitate thickness parameter points governing the thickness of the membrane core, it is necessary to recreate the membrane model with solid elements. In order to alleviate the peaks associated with problematic eigenfrequencies, a simple approach is used. Identify the first eigenfrequency not associated with rigid body motion ω_1 , and then maximize this eigenfrequency. Thus the objective function is a function that returns ω_1 for different design parameters x_k .

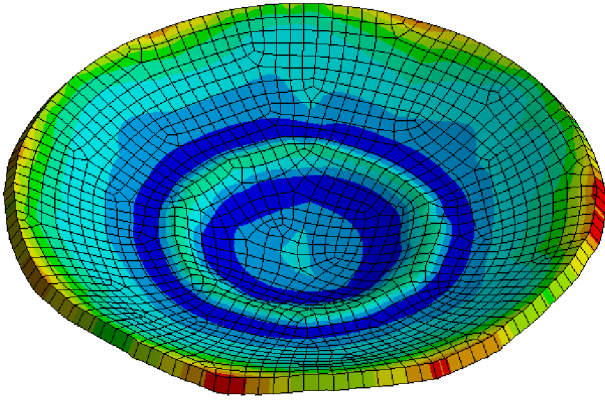


Fig. 11 Vibration mode corresponding to peak 6 at 4278 Hz.

$$\begin{aligned}
 & \underset{x_k}{\text{maximize}} && \omega_1(x_k) \\
 & \text{subject to} && \underline{x}_k \leq x_k \leq \bar{x}_k. \\
 & && g_1: M_{Total}(x_k) - 15.34 \text{ g} \leq 0
 \end{aligned} \tag{1}$$

The model of the membrane is parameterized in the CAD software SolidWorks as an axisymmetric drawing. Here, the shape of the top face sheet is kept constant. The core material of the membrane is defined by the top face sheet and spline 1 and the bottom face sheet is defined by spline 1 and 2. This axisymmetric drawing can be seen on Figure 12. The splines are defined by 5 points with equal angular spacing.

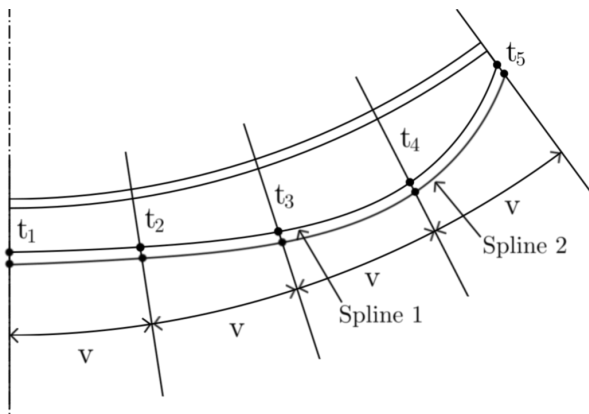


Fig. 12 Parameterization of core thickness.

This is illustrated in Figure 12, here the parameters t_k $k = 1, 2, 3, 4, 5$ define the thickness of the core material as defined from the center of curvature. These are chosen as the design parameters x_k . The thickness parameters are constrained by an upper bound, \bar{x} , of 10 mm and a lower bound, \underline{x} , of 1 mm determined from the geometric restrictions presented in subsection 1.1. The mass of the modelled membrane is 8.82 g and

to obtain an fundamental eigenfrequency of 38 Hz Børresen Acoustics adds an additional 6.52 g of epoxy to the voice coil. This additional mass could just as well be used to improve the frequency response of the membrane. Thus a constraint on the total mass of the membrane, $M_{Total}(x_k)$, of 15.34 g is added to the optimization problem.

ANSYS DesignXplorer is used to perform the optimization procedure of the membrane, by coupling DesignXplorer with a modal analysis of the membrane. Hereby, it is possible to maximize the eigenfrequencies of the membrane, in order to shift the eigenfrequencies outside of the upper limit of the operating range of the speaker driver. The DesignXplorer optimization algorithm used is a Nonlinear Programming by Quadratic Lagrangian (NLPQL). This is a gradient based single objective algorithm which generates new sample sets based on continuous input parameters. In order to calculate the gradients the algorithm implements a forward difference approximation [7].

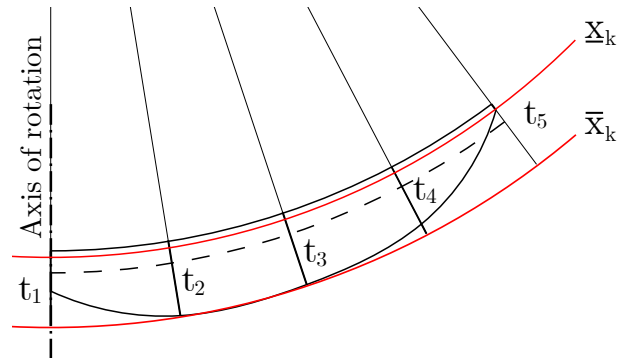


Fig. 13 Axisymmetric view of the optimized membrane (CP1), to scale. The dashed line marks the geometry of the reference geometry. The red lines mark the upper bound \bar{x}_k and lower bound \underline{x}_k .

Name	t_1 mm	t_2 mm	t_3 mm	t_4 mm	t_5 mm	Mass g	Freq Hz
Reference	3	3	3	3	3	8.04	1398
CP1	5.08	10	10	8.32	1	9.74	3123
CP2	4.67	10	10	6.76	1	9.43	3105

Tab. 4 Obtained values of the design parameters for the two candidate points calculated by the optimization analysis.

The result from the optimization analysis is two optimized geometries in the form of candidate points. The candidate points together with the reference is shown in Table 4.

The two candidate points obtain similar geometries for the membrane, in which the thickness of the membrane is decreased at the center and periphery of the membrane, and increased in the midway points from the center to the periphery, as illustrated in Figure 13, on which the reference geometry is depicted as a dashed line.

4.2 Results

The first candidate point (CP1) is implemented in the geometry of the membrane and a new modal analysis is performed, in order to determine the eigenfrequencies and their corresponding mode shapes of the optimized membrane. A cross sectional view of the reference geometry, Figure 14, and the optimized geometry, Figure 15, shows the difference in membrane geometry. The comparison of eigenfrequencies is listed in Table 5. The eigenfrequencies of the reference membrane, listed in Table 5, are lower than the eigenfrequencies obtained in subsection 2.1. This is a result of changes to the membrane model used for the optimization analysis. In order to facilitate the implementation of the thickness parameter points, it was not possible to use the shell model from subsection 2.1. Thus, the shell model needed to be recreated as a solid model, and as a result, it was not possible to use ANSYS ACP to create the membrane layout. Therefore, the material parameters do not correctly follow the geometry of the membrane, but instead follow the global coordinate system, which results in a discrepancy between the eigenfrequencies of the two models.

From Table 5 it is apparent that a significant shift in the eigenfrequencies of the membrane has been obtained. The first eigenfrequency of the membrane is shifted upwards by 124 % using a shape optimization, and as a result, the following eigenfrequencies has also been shifted upwards by a significant amount. The problematic eigenfrequencies and their corresponding mode shapes are tracked and highlighted by bold font. While the eigenfrequency of the problematic mode shape with four radial nodes observed at 1444 Hz in section 3 has been shifted upwards by 124 %, the eigenfrequency of the problematic mode shape with one concentric node observed at 4278 Hz in section 3 has been shifted downwards by 2.7 %. This is unexpected, due to the added thickness, and thus added stiffness, of the membrane. The added thickness of the membrane not only affects the first membrane eigenfrequency, of which the optimization is based, but also all following radial mode shapes.

Nr. (Rad,Con)	Freq. Ref. [Hz]	Freq. CP1 [Hz]	Difference
(4,0)	1398.7	3133	+1734.4(124%)
(6,0)	2481.4	5019.2	+2537.8(102%)
(8,0)	3599.3	6639.7	+3040.4(84%)
(10,0)	4458.9	8098	+3639.1(82%)
(12,0)	5378.2	9443.9	+4065.7(76%)
(14,0)	6271.2	10746	+4474.8(71%)
(16,0)	7145.2	-	-
(18,0)	8057	-	-
(0,1)	8123	7902.1	-220.9(-2.7%)
(2,1)	8454.4	9390.1	+935.7(11%)
(4,1)	8617.1	10869	+2251.9(26%)

Tab. 5 Comparison of the modal analysis of the reference membrane and optimized (CP1) membrane. Problematic eigenfrequencies are highlighted with bold font. Rad: Radial nodes, Con: Concentric nodes.

The possible cause of this phenomenon is further discussed in section 5.

The optimization of the membrane has not only affected the eigenfrequencies of the membrane itself but also the frequency response of the full assembly. The optimised membrane from candidate point CP1 is implemented in the full assembly, in order to evaluate whether the goal of shifting eigenfrequencies associated with the displacement peaks is accomplished. A harmonic analysis of the optimized full assembly is performed in the same frequency range as for the reference geometry, to determine the effect of the geometrical changes to the membrane and its impact on the frequency response of the full assembly. The full analysis can be found in the appendix report section 5.3.

The first membrane vibration mode with four radial nodes has been shifted upwards from 1444 Hz in the reference full assembly, to 2880 Hz in the optimized full assembly. As this is the first membrane eigenfrequency, no membrane vibration modes are present in the



Fig. 14 Cross sectional view of reference geometry of membrane.



Fig. 15 Cross sectional view of optimized geometry of membrane.

operating range of the speaker driver with the optimized geometry. Furthermore, the first concentric membrane vibration mode is identified in the optimized full assembly at a frequency of 4292 Hz, as illustrated by the red arrow on Figure 9, thereby roughly coinciding with the frequency of 4278 Hz at which it was identified in the reference full assembly, as illustrated by the black arrow. Thus, it supports the results of the modal analysis of the optimized membrane, in which the shape optimization yielded no significant shift in the eigenfrequency of the concentric vibration mode. Hereby, the optimization of the membrane has managed to shift all membrane eigenfrequencies of the membrane vibration modes entirely outside of the operating range of 0 Hz to 2500 Hz.

5. Discussion

The discussion will cover the material analysis, modal and harmonic analyses, modelling considerations, an alternative optimization formulation and finally manufacturing considerations.

For some of the materials it has been difficult to decide on the parameters, as no real data could be found. This is especially true for the surround where the variant of rubber is undisclosed, and the spider where different sources present material data of the spider with large deviations from one another. As a result of the range of material properties obtained for the spider, the stiffness of the spider is adjusted in order to exactly reproduce the fundamental eigenfrequency of the Børresen Acoustics speaker driver in the modelled full assembly.

From the modal analysis, it is apparent that a significant shift in the eigenfrequencies of the radial mode shapes has been achieved, with the first radial eigenfrequency shifted upwards by 124 %. One would also assume that the increased thickness of the optimized membrane would increase the eigenfrequencies of the concentric modes. However, the first concentric mode, with one concentric node, has remained largely unchanged, in fact with a small reduction of 2.7 %. This is likely explained by the honeycomb core of the membrane. Not only does the honeycomb structure not have the same stiffness in all directions, but it has a Poisson's ratio of 1, as mentioned in the appendix report section 3.1. This could explain the appearance of radial membrane mode shapes, despite having an axisymmetrically applied force, which should only excite concentric membrane mode shapes. As the honeycomb structure has a Poisson's ratio of 1, axisymmetric excitation causes

radial deformation, thus causing radial membrane mode shapes. Furthermore, the honeycomb core is not aligned with the radial and concentric directions. However, the phenomenon is also expected to be provoked by the asymmetric meshing of the models.

The vast majority of the vibration modes are solely due to the vibration of the surround alone. A possible solution to the abundance of surround vibration modes is to introduce a sorting of the mode shapes of the full assembly by using modal decomposition. Thus, one can decouple the system into its individual mode shapes, and thereby remove the non-physical surround vibration modes. The thorough analyses of the harmonic analyses will then be less time consuming and the identification of origins of displacement peaks more definite. Furthermore, if damping is implemented, the displacement peaks related to the surround vibration mode are expected to be reduced or suppressed entirely.

The current approach assumes that maximizing the eigenfrequency of the first membrane mode shape will result in an optimal membrane geometry for both the radial and concentric mode shapes. However, this is not expected to be the case. Changing this formulation would also solve the possible problem of non-differentiability of the objective function. A possible implementation of an optimization scheme that could increase the eigenfrequencies of both the radial and concentric mode shapes could be a bounded max-min, where the objective is to maximize the change in eigenfrequency of the first radial $\Delta\omega_{1Rad}$ and first concentric $\Delta\omega_{1Con}$.

$$\begin{aligned}
 & \underset{x_k, \beta}{\text{maximize}} && \beta \\
 & \text{subject to} && \underline{x}_k \leq x_k \leq \bar{x}_k. \\
 & && g_1: M_{Total}(x_k) - 15.34 \text{ g} \leq 0 \quad (2) \\
 & && g_2: \beta - \Delta\omega_{1Rad}(x_k) \leq 0 \\
 & && g_3: \beta - \Delta\omega_{1Con}(x_k) \leq 0
 \end{aligned}$$

Another possibility is to implement a Design Sensitivity Analysis (DSA), based on a finite difference of the mass and stiffness matrix, as formulated by [8]. This will decrease the number of eigenvalue problems solved.

Manufacturing considerations should be taken into account as the geometry of the membrane has changed after optimization. Care must be taken when draping the CSM face sheets on the optimized geometry because of the sharp point in the center of the membrane, which can be seen in Figure 15. When draping a

fiber composite laminate on a curved surface, the fiber orientation changes. If this is done to a significant extent, the material properties of the fiber composite laminate is altered. If the optimized membrane is to be implemented with a honeycomb core, the honeycomb core would have a varying thickness and still be draped on a double curved surface, introducing local buckling, which is described in the appendix report section 3.1. This will not allow for sufficient use of the properties of the honeycomb. Thus, the material of the membrane core should be changed. A material change of the core is, as described in Table 1, not a restriction, thus why, it is proposed to change the material of the membrane core. Changing the core material is expected to affect the result of the optimized geometry. A material that can replace the honeycomb is polyvinylchlorid (PVC) foam. One of the benefits of using PVC foam is, that the density of the foam core can be altered to match the exact requirements for the speaker driver in order to obtain the wanted fundamental eigenfrequency. Thus, there is no longer a reason for adding mass to the finished membrane, in order to obtain the wanted fundamental eigenfrequency. Furthermore, the foam core has isotropic material properties, and more importantly, a Poisson's ratio of approximately 0.32 [9], thus why the added thickness of the membrane is expected to now also affect the eigenfrequencies of the concentric membrane mode shapes. The use of a foam core will also introduce damping to the membrane which could lower or entirely suppress the magnitude of the membrane vibration modes.

6. Conclusion

From the isolated modal analysis of the membrane, it was possible to identify vibration modes in the full assembly, with origin in membrane mode shapes. Two distinct displacement peaks in the frequency response of the full assembly are observed at 1444 Hz and 4278 Hz, the origins of which are a membrane vibration mode with four radial nodes and a membrane vibration mode with one concentric node respectively. These problematic membrane eigenfrequencies and associated mode shapes are the proposed origins of the impedance peaks at 1625 Hz and 3979 Hz in Figure 3.

By a shape optimization of the membrane it was possible to obtain a significant shift in the eigenfrequencies of the membrane. While the eigenfrequency of the problematic mode shape with four radial nodes observed at 1444 Hz was shifted upwards by 124 %, the eigenfrequency of the problematic mode shape with one

concentric node observed at 4278 Hz was unaffected and has in fact been shifted downwards by 2.7 %.

When the optimized membrane was implemented in the full assembly the problematic membrane vibration mode with four radial nodes was shifted upwards from 1444 Hz in the reference full assembly, to 2880 Hz in the optimized full assembly. Thus, it is shifted outside the operating range of the speaker driver of 2500 Hz. As this is the first eigenfrequency of the optimized membrane, no membrane vibration modes now exist in the operating range of the speaker driver. The problematic membrane vibration mode with one concentric node was moved from 4278 Hz to 4292 Hz, thereby roughly coinciding with the frequency identified in the reference full assembly.

The change in geometry from the optimization, together with the material analysis of the honeycomb in the appendix report section 3.1, show that in order to implement the optimized geometry, the core material of the membrane must be changed. This might have a beneficial influence on the shift in eigenfrequencies from the optimization, as the material parameters will change and the Poisson's ratio will be lower than 1. This could therefore affect the concentric mode shape.

In order to compare the model to the Børresen speaker driver, the model should be verified experimentally.

Acknowledgement

The authors of this work gratefully acknowledge Grundfos for sponsoring the 9th MechMan symposium.

References

- [1] Børresen Acoustics ApS, "Børresen 0-series technology." <https://borresen-acoustics.com/index.php/the-speakers/borresen-0-series-technology>. [Online; accessed 2021-03-10].
- [2] V. Dickason, "*Loudspeaker Design Cookbook*". Audio Amateur Press, 2006.
- [3] N. W. McLachlan, "*Loud Speakers Theory Performance, Testing and Design*". Oxford University Press, 1934.
- [4] G. Hill, "*Loudspeaker Modelling and Design*". Taylor and Francis, 2019.
- [5] D. Henwood and G. Geaves, "Finite Element Modelling of a Loudspeaker Part 1: Theory and Validation" 2005.
- [6] Y. Shiozawa, H. Onitsuka, H. Nakashima, and K. Fukatsu, "A multi-physical loudspeaker model including breakup membrane modes" 2016.
- [7] ANSYS, "DesignXplorer User's Guide" 2020.
- [8] A. P. Seyranian, E. Lund, and N. Olhoff, "Multiple eigenvalues in structural optimization problems" vol. 8, 1994.
- [9] Matweb, "Overview of materials for pvc, foam grade." http://www.matweb.com/search/datasheet_print.aspx?matguid=e19bc7065d1c4836a89d41ff23d47413, 2021. [Online; accessed 2021-05-21].